Uniport Journal of Engineering and Scientific Research (UJESR)

Vol. 7, Issue 1, 2022, Page 31-38
ISSN: 2616-1192

(www.ujesr.org)

Predicting Abrasive Wear Distribution in Hot Forging Dies

Ebojoh, E*[1] and Amgbari, C.O[2]
[1]Department of Production Engineering, University of Benin
[2]Department of Mechanical Engineering Technology Federal Polytechnic Ekowe, Bayelsa state.
*Corresponding author's email: voke.ebojoh@uniben.edu

Abstract
This paper presents an examination of the wear distribution set up at various points in a die during forging operation by the finite element method. This paper presents the numerical solution to the one-dimensional time dependent differential equation which describes the pressure exerted by forging on a die. In conducting the analysis, the blank was split into a finite number of elements and the Galerkin finite element method was applied to obtain the weighted integral form. The finite element model was then developed and solved to obtain the pressures and stress in an open die forging operation. The results obtained from the present study were compared with the exact solution they were found to be almost identical while the FEM approximates the exact solution for both the quadratic and linear elements graphically. It was observed that the model fits in well with a coefficient of determination (R^2) of 99.8%.
Keywords: *Galerkin finite element, Wear Distribution, Forging, Die radius*

Received: 30th July, 2022 *Accepted: 29th September, 2022*

1. Introduction

The forging process is a massive forming process, characterized by the application of a high compressive load which generates plastic strain of the billet (Altan, 2005). Claudio (2015) also carried out a comparative study of different artificial intelligence techniques to map an input-output relationship of a manufacturing process and optimize the desired responses. These techniques were used to model and optimize the impression die forging process. Stahlberg and Hallstrom (1999) further showed that 70% of tool replacements were due to premature die wear, another 25% were due to mechanical fatigue and the remaining 5% were due to plastic deformation and thermal-mechanical fatigue. They concluded the die wear is the dominant tool failure factor for the forging tool replacement during mass production. Also, the amount of wear in dies can be forecasted using a proposed model which composed of the cumulative friction work of the metal flow on the surfaces of the dies and the yield strengths of the die materials at elevated temperatures (Toshiaki, 2017). Also, Oviawe et al. (2018) investigated the abrasive wear distribution in a forging die under constant dimensional wear coefficient. The abrasive wear differential governing equation was used in the analysis. The finite element technique, using quadratic shape interpolation functions elements was employed to carry out the analysis over the cross-section of the die which involves discretizing the domain into finite element, analyzing this finite element, assembling the results from the analysis of the analyzed finite element, imposing the boundary conditions and finally, getting the results that represent the entire domain. A better way of studying abrasive wear is in terms of the specific energy and the energy equation required to removing a unit volume of material (Shaw, 2005).

2. Materials and methods

2.1 Numerical solution

The model developed by Ebojoh and Amgbari (2018) which takes into account the deformation energy, sliding velocity and coefficient of friction of the die material and other associated parameters is as presented in Equation (1).

$$\frac{d^2B}{dv^2}+\frac{dB}{dv}-\frac{\mu}{u}m=\frac{m}{F}\left(\frac{dB}{dt}\right) \quad (1)$$

where B = Wear module (mm), L = Distance traveled by abrasive particle (ds) (mm), F = Applied force (N), μ = Coefficient of friction, and u = Specific energy to produce a chip MPa.

2.2 Finite element formulation

The weak form of Equation (1) is obtained by multiplying Equation (1) with a weight function of w (t) and integrating over the domain of the entire element with the following initial and boundary conditions:

$B(0,t) = 0$ and $\frac{dB}{dt}(v,t) = 0$ (2)

Initial condition: $B(v,0) = B_o$ (3)

$$\int_v w(t)\frac{d^2B}{dv^2}dv + \int_v w(t)\frac{dB}{dv}dv - \frac{m}{F}\int_v w(t)\frac{dB}{dt}dv - \frac{\mu m}{u}\int_v w(t)dv = 0 \quad (4)$$

Equation (4) becomes:

$$\int_v \frac{dw}{dv}\bullet\frac{dB}{dv}dv + \int_v w(t)\frac{dB}{dv}dv - \frac{m}{F}\int_v w(t)\frac{dB}{dt}dv - \frac{\mu m}{u}\int_v w(t)dv - \left[w(t)\frac{dB}{dv}\right]_v = 0 \quad (5)$$

Since Equation (5) is in coupled variable form, we need to decouple the solution by assuming that

$B(v,t) \approx B^e(v,t) = \sum_{j=1}^{n} B_j^e(t)\psi_j^e(v)$ (6)

and

$w(t) = \psi_i^e(t)$ (7)

where ψ_{ij}^e is the shape function of interpolation at i, j nodes and B_{ij}^e is the wear depth (module) at i, j nodes of the element. Substituting Equations (6) and (7) into Equation (5):

$$\int_v \frac{d\psi_i^e}{dv}\bullet\frac{d\sum_{j=1}^{n} B_j^e(t)\psi_j^e(v)}{dv}dv + \int_v \psi_i^e(t)\frac{d\sum_{j=1}^{n} B_j^e(t)\psi_j^e(v)}{dv}dv - \frac{m}{F}\int_v \psi_i^e(t)\frac{d\sum_{j=1}^{n} B_j^e(t)\psi_j^e(v)}{dt}dv - \frac{\mu m}{u}\int_v \psi_i^e(t)dv - \left[\psi_i^e(t)\frac{d\sum_{j=1}^{n} B_j^e(t)\psi_j^e(v)}{dv}\right]_v = 0 \quad (8)$$

Simplifying further

$$B_j\int_v \frac{d\psi_i^e}{dv}\bullet\frac{d\psi_j^e}{dv}dv + B_j\int_v \psi_i^e(t)\frac{d\psi_j^e}{dv}dv - \frac{m}{F}\int_v \psi_i^e\psi_j^e(t)\frac{dB}{dt}dv - \frac{\mu m}{u}\int_v \psi_i^e(t)dv - B_j\left[\psi_i^e(t)\frac{d\psi_j^e}{dv}\right]_v = 0 \quad (9)$$

let

$$K = \int_v \left[\left(\frac{d\psi_i^e}{dv}\bullet\frac{d\psi_j^e}{dv}\right) + \left(\psi_i^e(t)\frac{d\psi_j^e}{dv}\right)\right]dv \quad (10)$$

$$M = \int_v \psi_i^e\psi_j^e(t)dv \quad (11)$$

$$F = \int_v \psi_i^e dv \quad (12)$$

$$Q = B\left[\psi_i^e(t)\frac{d\psi_j^e}{dv}\right]_v \quad (13)$$

In linear form, the semi-discrete finite element model can be represented as:

$$\left[K_{ij}^e\right]\{B\} - \frac{m}{F}\left[M_{ij}^e\right]\left\{\dot{B}\right\} - \frac{\mu m}{u}\left[F_{ij}^e\right] = \{Q^e\} \quad (14)$$

Using Quadratic Lagrange Interpolation functions for a quadratic element:

$$\psi_1 = \left(1 - \frac{v}{B_e}\right)\left(1 - \frac{v}{B_e}\right) \tag{15}$$

$$\psi_2 = \frac{4v}{B_e}\left(1 - \frac{v}{B_e}\right) \tag{16}$$

$$\psi_3 = \left(-\frac{v}{B_e}\right)\left(1 - \frac{2v}{B_e}\right) \tag{17}$$

The wear coefficient matrix (K), the wear mass matrix (M) and the flux matrix (F) can easily be derived by substituting the Lagrange interpolation functions of Equations (15) to (17) into Equations (10) to (13), respectively. The coefficient matrix can easily be derived by substituting the shape interpolation functions into Equation (10).

$$\left[k_{ij}^e\right] = \frac{1}{3B_e}\begin{bmatrix} 7 & -8 & 1 \\ -8 & 16 & -8 \\ -1 & 8 & -7 \end{bmatrix} + \frac{1}{6}\begin{bmatrix} -3 & 4 & -1 \\ -4 & 0 & 4 \\ 1 & -4 & 3 \end{bmatrix} \tag{18}$$

Also, the mass matrices can easily be derived by substituting the shape functions into Equation (11).

$$\left[M_{ij}^e\right] = \frac{mB}{30F}\begin{bmatrix} 4 & 2 & 1 \\ -2 & 16 & 2 \\ -1 & -2 & -4 \end{bmatrix} \tag{19}$$

Similarly, for the source vector matrix was derived by substituting the shape functions into Equation (12). The matrices are shown below:

$$\{F_i^e\} = \frac{\mu mB}{6u}\begin{Bmatrix} 1 \\ 4 \\ 1 \end{Bmatrix} \tag{20}$$

In this analysis, the computational details of shape assembly of finite element analysis (FEA) used is found in Reddy (1993 and 2006). However the assembly matrices are presented in Equations (21) to (25).

$$[K^e] = \begin{bmatrix} K_{11}^1 & K_{12}^1 & K_{13}^1 & 0 & 0 & 0 & 0 & 0 & 0 \\ K_{21}^1 & K_{22}^1 & K_{23}^1 & 0 & 0 & 0 & 0 & 0 & 0 \\ K_{31}^1 & K_{32}^1 & K_{33}^1 + K_{11}^2 & K_{12}^2 & K_{13}^2 & 0 & 0 & 0 & 0 \\ 0 & 0 & K_{21}^2 & K_{22}^2 & K_{23}^2 & 0 & 0 & 0 & 0 \\ 0 & 0 & K_{31}^2 & K_{32}^2 & K_{33}^2 + K_{11}^3 & K_{12}^3 & K_{13}^3 & 0 & 0 \\ 0 & 0 & 0 & 0 & K_{21}^3 & K_{22}^3 & K_{23}^3 & 0 & 0 \\ 0 & 0 & 0 & 0 & K_{31}^3 & K_{32}^3 & K_{33}^3 + K_{11}^4 & K_{12}^4 & K_{13}^4 \\ 0 & 0 & 0 & 0 & 0 & 0 & K_{21}^4 & K_{22}^4 & K_{23}^4 \\ 0 & 0 & 0 & 0 & 0 & 0 & K_{31}^4 & K_{32}^4 & K_{33}^4 \end{bmatrix} \tag{21}$$

$$[M^e] = \begin{bmatrix} M_{11}^1 & M_{12}^1 & M_{13}^1 & 0 & 0 & 0 & 0 & 0 & 0 \\ M_{21}^1 & M_{22}^1 & M_{23}^1 & 0 & 0 & 0 & 0 & 0 & 0 \\ M_{31}^1 & M_{32}^1 & M_{33}^1 + M_{11}^2 & M_{12}^2 & M_{13}^2 & 0 & 0 & 0 & 0 \\ 0 & 0 & M_{21}^2 & M_{22}^2 & M_{23}^2 & 0 & 0 & 0 & 0 \\ 0 & 0 & M_{31}^2 & M_{32}^2 & M_{33}^2 + M_{11}^3 & M_{12}^3 & M_{13}^3 & 0 & 0 \\ 0 & 0 & 0 & 0 & M_{21}^3 & M_{22}^3 & M_{23}^3 & 0 & 0 \\ 0 & 0 & 0 & 0 & M_{31}^3 & M_{32}^3 & M_{33}^3 + M_{11}^4 & M_{12}^4 & M_{13}^4 \\ 0 & 0 & 0 & 0 & 0 & 0 & M_{21}^4 & M_{22}^4 & M_{23}^4 \\ 0 & 0 & 0 & 0 & 0 & 0 & M_{31}^4 & M_{32}^4 & M_{33}^4 \end{bmatrix} \tag{22}$$

$$F_i \text{ matrix} \qquad \{F_i^e\} = \begin{Bmatrix} F_1^1 \\ F_2^1 + F_2^2 \\ F_3^2 + F_2^3 \\ F_4^3 + F_4^4 \\ F_5^4 + F_5^5 \\ F_6^5 + F_6^6 \\ F_7^6 + F_7^7 \\ F_8^7 + F_8^8 \\ F_9^8 \end{Bmatrix} \tag{23}$$

Due to balance of internal fluxes:

$$\begin{aligned} &Q_2^1 + Q_2^2 = Q_4^3 + Q_4^4 = Q_6^5 + Q_6^6 = Q_8^7 + Q_8^8 = 0 \\ &Q_3^2 + Q_3^3 = Q_5^4 + Q_5^5 = Q_7^6 + Q_7^7 = 0 \end{aligned} \tag{24}$$

$$Q_i \text{ matrix} \quad \{Q_i^e\} = \begin{Bmatrix} Q_1^1 \\ Q_2^1 + Q_2^2 \\ Q_3^2 + Q_2^3 \\ Q_4^3 + Q_4^4 \\ Q_5^4 + Q_5^5 \\ Q_6^5 + Q_6^6 \\ Q_7^6 + Q_7^7 \\ Q_8^7 + Q_8^8 \\ Q_9^8 \end{Bmatrix} \tag{25}$$

$$\frac{1}{3B_e}\begin{bmatrix} \frac{13}{2} & \frac{-22}{3} & \frac{5}{6} & 0 & 0 & 0 & 0 & 0 & 0 \\ \frac{-26}{3} & 16 & \frac{-22}{3} & 0 & 0 & 0 & 0 & 0 & 0 \\ \frac{-5}{6} & \frac{22}{3} & 0 & \frac{-22}{3} & \frac{5}{6} & 0 & 0 & 0 & 0 \\ 0 & 0 & \frac{-26}{3} & 16 & \frac{-22}{3} & 0 & 0 & 0 & 0 \\ 0 & 0 & \frac{-5}{6} & \frac{22}{3} & 0 & \frac{-22}{3} & \frac{5}{6} & 0 & 0 \\ 0 & 0 & 0 & 0 & \frac{-26}{3} & 16 & \frac{-22}{3} & 0 & 0 \\ 0 & 0 & 0 & 0 & \frac{-5}{6} & \frac{22}{3} & 0 & \frac{-22}{3} & \frac{5}{6} \\ 0 & 0 & 0 & 0 & 0 & 0 & \frac{-26}{3} & 16 & \frac{-22}{3} \\ 0 & 0 & 0 & 0 & 0 & 0 & \frac{-5}{6} & \frac{22}{3} & \frac{-13}{2} \end{bmatrix}\begin{bmatrix} B_1 \\ B_2 \\ B_3 \\ B_4 \\ B_5 \\ B_6 \\ B_7 \\ B_8 \\ B_9 \end{bmatrix} + \frac{mB_e}{30F}\begin{bmatrix} 4 & 2 & 1 & 0 & 0 & 0 & 0 & 0 & 0 \\ 2 & 16 & 2 & 0 & 0 & 0 & 0 & 0 & 0 \\ -1 & -2 & 0 & 2 & 1 & 0 & 0 & 0 & 0 \\ 0 & 0 & 2 & 16 & 2 & 0 & 0 & 0 & 0 \\ 0 & 0 & -1 & -2 & 0 & 2 & 1 & 0 & 0 \\ 0 & 0 & 0 & 0 & 2 & 16 & 2 & 0 & 0 \\ 0 & 0 & 0 & 0 & -1 & -2 & 0 & 2 & 1 \\ 0 & 0 & 0 & 0 & 0 & 0 & 2 & 16 & 2 \\ 0 & 0 & 0 & 0 & 0 & 0 & -1 & -2 & -4 \end{bmatrix}\begin{bmatrix} \dot{B}_1 \\ \dot{B}_2 \\ \dot{B}_3 \\ \dot{B}_4 \\ \dot{B}_5 \\ \dot{B}_6 \\ \dot{B}_7 \\ \dot{B}_8 \\ \dot{B}_9 \end{bmatrix} = \frac{\mu mB}{6u}\begin{Bmatrix} 2 \\ 4 \\ 2 \\ 4 \\ 4 \\ 2 \\ 4 \\ 4 \\ 1 \end{Bmatrix} + \begin{Bmatrix} Q_1^1 \\ 0 \\ 0 \\ 0 \\ 0 \\ 0 \\ 0 \\ 0 \\ Q_9^8 \end{Bmatrix} \tag{26}$$

2.3 Time approximation for abrasive wear

In this study, a time approximation is adopted, using α-family of interpolation (Reddy, 1993 and 2006). Recall that Equation (17) is of the form:

$$\left[K_{ij}^e\right]\{B\} - \frac{m}{F}\left[M_{ij}^e\right]\left\{\dot{B}\right\} - \frac{\mu m}{u}\left[F_{ij}^e\right] - [Q^e] = 0 \tag{27}$$

For a given time step s, Equation (17) becomes

$$\left[K_{ij}^e\right]\{B\}_s - \frac{m}{F}\left[M_{ij}^e\right]\left\{\dot{B}\right\}_s = \frac{\mu m}{u}\left[F_{ij}^e\right]_s + [Q^e]_s \tag{28}$$

For the next time step $s+1$, Equation (27) becomes

$$\left[K_{ij}^{e}\right]\{B\}_{s+1} - \frac{m}{F}\left[M_{ij}^{e}\right]\left\{\dot{B}\right\}_{s+1} = \frac{\mu m}{u}\left[F_{ij}^{e}\right]_{s+1} + [Q^{e}]_{s+1} \quad (29)$$

Applying the Crank-Nicholson finite differences scheme and taking (α=0.5) and a time step $(\Delta t = 0.005)$ and applying the various steps in Reddy (1993 and 2006) the depth of wear is computed as shown in Equation (30).

$$\{B\}_{s+1} = \left[\left[M_{ij}^{e}\right] + \frac{\Delta t}{2}\left[K_{ij}^{e}\right]\right]^{-1} \bullet \left[\left[\left[M_{ij}^{e}\right] - \frac{\Delta t}{2}\left[K_{ij}^{e}\right]\right]\{B\}_{s} + \frac{\Delta t \mu m}{2u}\left[F_{ij}^{e}\right] + \Delta t\{Q_{i}^{e}\}\right] \quad (30)$$

3. Results and discussion

A software programming code was used to obtain wear depth of the die in Matlab (2015). The parameters affecting the wear depth are presented in Table 1 which were inputted in Equation (30) via the code. Table 2 shows the comparison between wear depth of finite element analysis for the quadratic element, the linear element and exact solution. It is observed that the results of the analysis approximate faster to the exact solution. As the numbers of elements are increased the accuracy also increases.

Table 1: Parameters for calculating wear distribution in forge die

Parameter	Value
Sliding distance (s)	2mm
Mass of hammer (m)	4.5kg
Contact force (F)	100N
Initial Temperature of work piece (T)	1100 ^{o}C
Initial Temperature of die	300 ^{o}C
α-family	0.5
Time-step (Δt)	0.005
Coefficient of friction (μ)	0.3

Table 2: Wear depth distribution in the forge die

Radius	Wear Depth (mm)		
(mm)	Quadratic element	Linear element	Exact solution
0.0000	0.1000	0.1000	0.1000
0.1250	0.1820	0.2022	0.1921
0.2500	0.2112	0.2038	0.2975
0.3750	0.3555	0.3550	0.3430
0.5000	0.4479	0.4504	0.4492
0.6250	0.5209	0.5223	0.5216
0.7500	0.5855	0.5861	0.5858
0.8750	0.6420	0.6424	0.6424
1.0000	0.6896	0.6901	0.6899
1.1250	0.7287	0.7295	0.7290
1.2500	0.7687	0.7612	0.7650
1.3750	0.7856	0.7864	0.7861
1.5000	0.8049	0.8058	0.8054
1.6250	0.8191	0.8199	0.8201
1.7500	0.8286	0.8294	0.8290
1.8750	0.8339	0.8348	0.8341
2.0000	0.8356	0.8366	0.8361

Fig. 1 is the plot of wear depth against contact die radius. It is observed that at radii of 0.125 mm to 0.25mm there was a contour during the forging process and this may be as a result of the value u the specific energy to produce a chip in MPa, however, there was steady depth and rate of cut thereafter as shown. Fig. 3 shows a deeper contour or chip formation at that point due to its linearity. From Fig. 2 and Fig. 4, it was observed that the result of the finite element analysis approximates better to the exact solution. And when compared together, that is the quadratic, linear and exact solution, the comparison shows a strong positive correlation as shown in Fig. 5.

It was observed using the MiniTab (14) software that the model fits in well with a coefficient of determination (R^2) of 99.8%. This shows that the FEA was able to account for 99.8% of the variation in the given period of 2mm radius. The estimated standard deviation (S) of the error in this model is 0.0165661. The Degree of Freedom (DF) which indicates the number of independent pieces of information involving the response data needed to calculate the sum of squares for the regression was calculated to be 1 while that of the error was calculated to be 5 with a total DF of 6. Also the total sum of squared (SS) distance was calculated to be approximately 0.180696. From this, the SS Regression which was a portion of the variation explained by the model, was estimated to be 0.179324 while the SS Error which was the portion not explained by the model and was therefore attributed to the errors, was estimated to be 0.001372. The Mean Square Regression (MSR) of the model was estimated to be 0.179324 while the Mean Square of the Error (MSE) also known as Mean Squared Deviation (MSD) which is a risk function was estimated to be 0.000274.

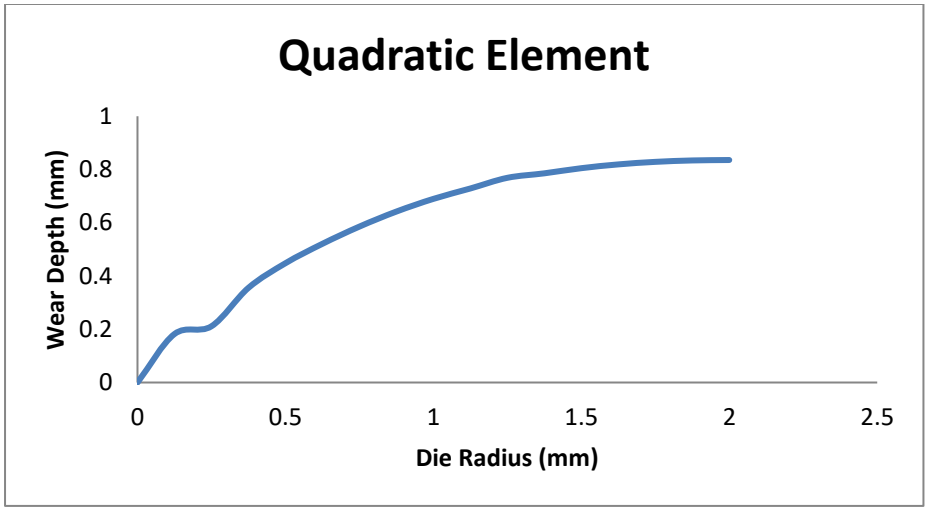

Fig. 1: Wear depth against die radius (FEA)

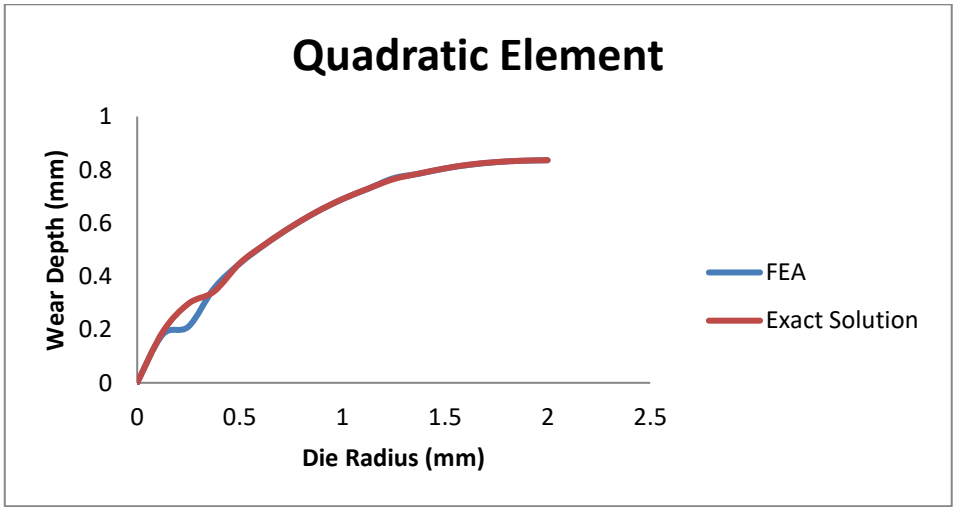

Fig. 2: Wear depth against die radius (FEA/EXACT)

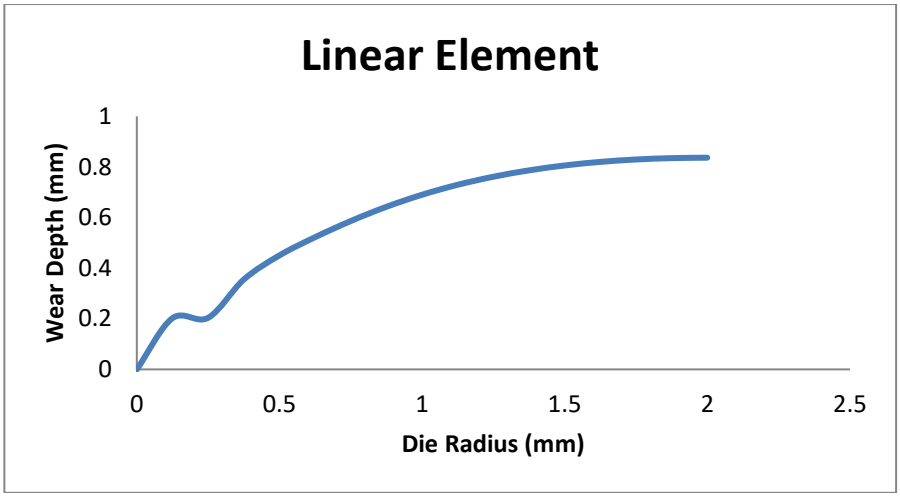

Fig. 3: Wear depth against die radius (FEA)

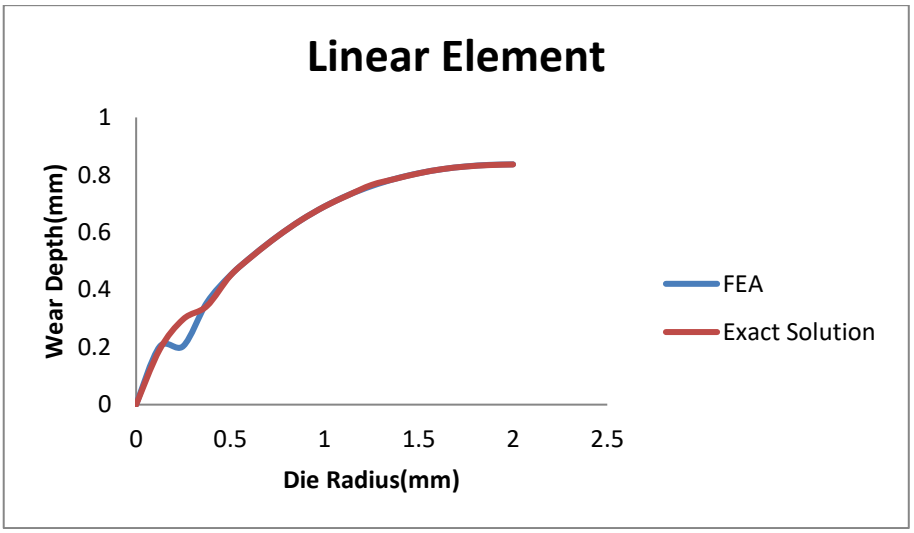

Fig. 4: Wear depth against die radius (FEA/EXACT)

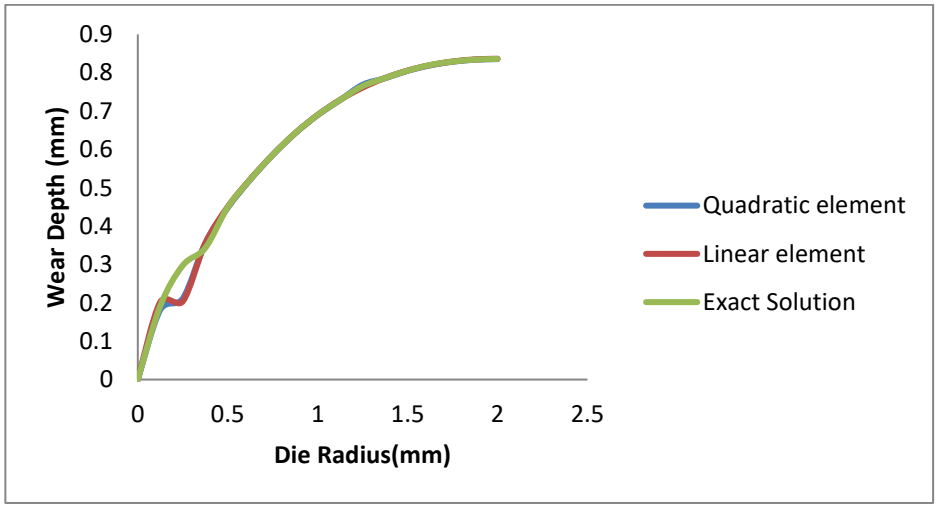

Fig. 5: Wear depth against die radius

4. Conclusion

This paper has able to present the prediction of abrasive wear in hot forging die using the Galerkin's Finite element method. The accuracy of the FEA solution compared with the exact result show a strong positive agreement which is an indication that this analysis is of higher accuracy and efficiency to predict abrasive wear in hot forging dies.

References

Altan, T. (2005) Cold and hot forging: fundamentals and applications. ASM international, 2005.

Claudio, C., Teresa, C., Giuseppina, A., Luigi, F. and Roberto, M. (2015) Design of a high-performance predictive tool for forging operation. Procedia CIRP, 33(2015):173-178.

Ebojoh, E. and Amgbari, C. (2018) Proposed Model for Predicting Abrasive Wear in Hot Forging Dies. International Journal of Advanced Engineering and Technology, 2(2):72-73.

Oviawe, C.I., Akpobi, J.A. and Oviawe, O. (2018) Analysis and Prediction of Die Wear in Hot Forging Operation. The Journal of the Nigerian Institution of Production Engineers, 22:216-224.

Reddy, J.N. (1993) An introduction to the finite element method, McGraw-Hill, 2nd edition, pp. 117-599.

Reddy, J.N. (2006) An introduction to the finite element method, McGraw-Hill, 2nd edition, pp. 146-442.

Shaw, M.C. (2005) Metal cutting principles. Oxford Science Publishers, 170-175.

Stahlberg, U. and Hallstrom, J. (1999) A comparison between two wear models. J. Materials Processing Technology, 87(1999):223-229.

Toshiaki, T., Koukichi, N., Yasuhiro, Y., Sayuri, K., Yoshinari, T., Toshiyuki, S. and Atsuo, W. (2017) Prediction of Hot Forging Die Life Using Wear and Cooling. R&D Review of Toyota CRDL 40 No.1.